

# Self-Sensitized Fulgimides with Selective Multiplicity-Based Three-State Photoswitching

Jakub Copko,<sup>[a]</sup> Lucie Ludvíková,<sup>[a]</sup> and Tomáš Slanina\*<sup>[a]</sup>

Precise control over excited-state multiplicity is a powerful strategy for controlling photochemical reactivity, particularly in multimodal systems where different multiplicities lead to distinct reaction products. Here, we present a multiplicity-sensitive, multimodal, fulgimide-based system capable of three-state photoswitching both in solution and in the solid state. With the aim of suppressing singlet-state sensitization, we rationally

designed an intramolecularly sensitized system that enables triplet-exclusive energy transfer—a crucial feature for selective multiplicity-dependent reactivity. Our findings provide insights into the underlying principles of intramolecular triplet-exclusive sensitization and its application in controlling three-state photoswitching in unimolecular systems.

## 1. Introduction

Achieving selective chemical reactivity is fundamental for the precise formation of new compounds. Though chemical reactivity is governed by various factors, including the nature of the reactants, reaction conditions, and the presence of catalysts, a single set of reactants can result in multiple reaction pathways, yielding a variety of products. This underscores the need for a deeper understanding of these factors in order to effectively steer reaction conditions toward desired outcomes. An example of how chemical reactivity can be influenced by the electronic nature of a reactant is demonstrated in the chemistry of carbenes.<sup>[1–3]</sup> Carbenes add to alkenes via two mechanisms: a concerted pathway for singlet carbenes and a stepwise pathway for triplet carbenes, leading to different distributions of cyclopropane products. In this scenario, the multiplicity of the reagent exerts strict control over chemical reactivity.

While multiplicity-based control of organic molecules is rare in the ground state since they mostly exist as singlets, the excited state offers greater opportunities, as electronically excited molecules can exist in either a singlet or triplet excited state.<sup>[4]</sup> By understanding the unique properties of excited states, chemists can further refine their ability to control the outcomes of photophysical and chemical processes. Stilbene exemplifies multiplicity-controlled photoreactivity. Though not being the most stable isomer, the *Z*-form of stilbene follows one of

two reaction pathways: double-bond isomerization yielding the *E*-form or  $6\pi$ -electrocyclization forming dihydrophenanthrene (Scheme 1, top).<sup>[5–7]</sup>

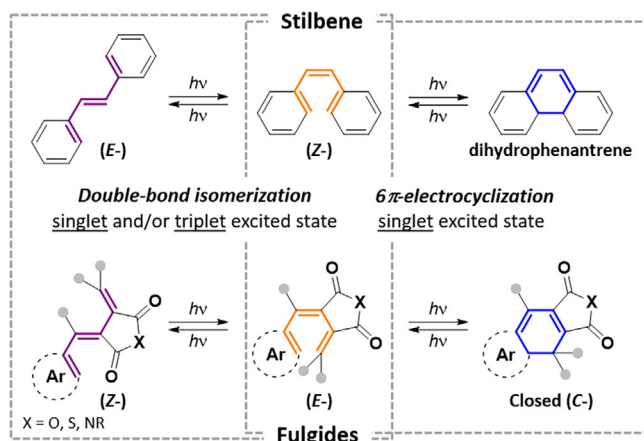
Photo-initiated  $6\pi$ -electrocyclization follows spin selection rules, proceeding from the singlet excited state via excited-state-allowed conrotatory motion, as per Woodward–Hoffmann rules.<sup>[8–11]</sup> In contrast, double-bond isomerization is independent of excited-state multiplicity and can occur through the singlet state, the triplet state, or a combination of both.<sup>[5,12–14]</sup> On the singlet excited-state energy surface, the local minima of both *E*- and *Z*-isomers exhibit geometries similar to their ground-state counterparts, while the energy barrier for their interconversion is greatly reduced.<sup>[15,16]</sup> Therefore, the system can undergo adiabatic isomerization on the singlet excited-state hypersurface, establishing an equilibrium between *E*- and *Z*-isomers. This equilibrium resembles the relative energetic positions of their ground-state energies. Direct irradiation to a photostationary state (PSS), where each isomer has the same photochemical driving force (extinction coefficient multiplied by the corresponding quantum yield), will preferentially yield the *E*-form.<sup>[17,18]</sup> In the vertically excited triplet state of either the *Z*- or *E*-isomer, relaxation leads to a twisted geometry state ( $\sim 90^\circ$  dihedral angle),<sup>[12]</sup> formerly known as the phantom triplet state (Scheme 2). While the ground-state energy reaches a maximum at a  $90^\circ$  dihedral angle, the twisted triplet state corresponds to a minimum on the triplet energy surface. The triplet excited-state hypersurface intersects with the ground-state hypersurface near the phantom triplet state, leading to rapid deexcitation by intersystem crossing (ISC) from the triplet excited state to the ground state.<sup>[7,15,19,20]</sup>

Though the minimum energy triplet geometry is the same for both isomers, the vertically excited triplet state of the *E*-form typically has to overcome a barrier before reaching the twisted minimum. In contrast, the *Z*-form twists via either a lower barrier or a barrier-free path on the triplet hypersurface. The presence of the barrier is indirectly observed through variations in triplet excited-state lifetimes; the  $\tau_T$  of the *E*-form is typically 1–3 ns longer than that of the *Z*-form in various solvents.<sup>[21,22]</sup>

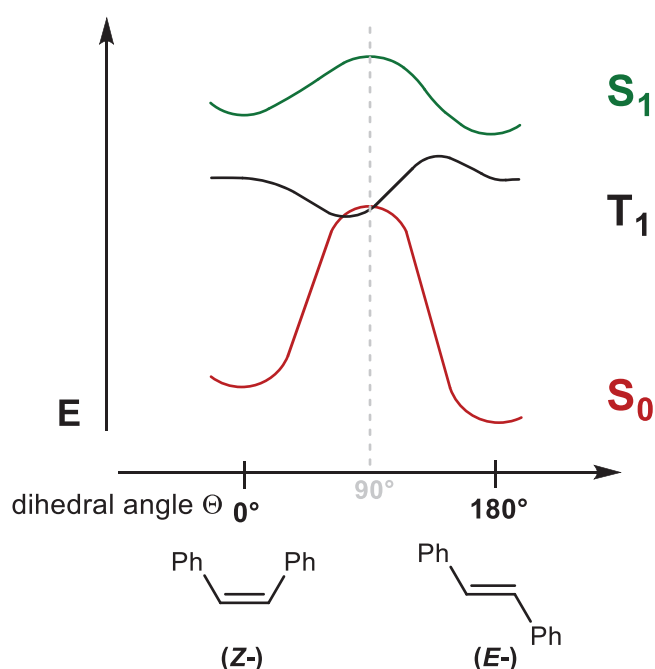
[a] J. Copko, L. Ludvíková, T. Slanina  
Institute of Organic Chemistry and Biochemistry of the Czech Academy of Sciences, Flemingovo náměstí 542/2, Prague 6, 160 00, Czech Republic  
E-mail: tomas.slantina@uochb.cas.cz

Supporting information for this article is available on the WWW under <https://doi.org/10.1002/chem.202500678>

© 2025 The Author(s). Chemistry – A European Journal published by Wiley-VCH GmbH. This is an open access article under the terms of the Creative Commons Attribution-NonCommercial License, which permits use, distribution and reproduction in any medium, provided the original work is properly cited and is not used for commercial purposes.



**Scheme 1.** Excited-state multiplicity-dependent photoinduced isomerizations of stilbenes (top) and fulgides (bottom).



**Scheme 2.** Representation of the potential energy surface of the ground-state ( $S_0$ ), singlet ( $S_1$ ), and triplet ( $T_1$ ) excited states of stilbene along the double bond rotation, specified by the dihedral angle  $\theta$ . The twisted geometry state (phantom triplet) is the minimum on the  $T_1$  hypersurface near the 90° dashed line (in gray).

Due to the presence of this barrier, the phantom triplet-state geometry shifts slightly toward the Z-form.<sup>[23]</sup> Similarly, the intersection with  $S_0$  and, as a result, the de-excitation from the phantom triplet state, is nonsymmetric, preferring relaxation toward the Z-form.<sup>[24,25]</sup> Stilbenes can be therefore identified as a rare example where solely the multiplicity of the excited state governs the selectivity of photoinduced isomerizations, thus enabling external control. Typically, the singlet excited state is attained through direct excitation, whereas the triplet excited state is achieved via triplet photosensitization.<sup>[26,27]</sup>

While the photoswitching of stilbenes can be controlled by multiplicity, their practical use is limited by their thermal and

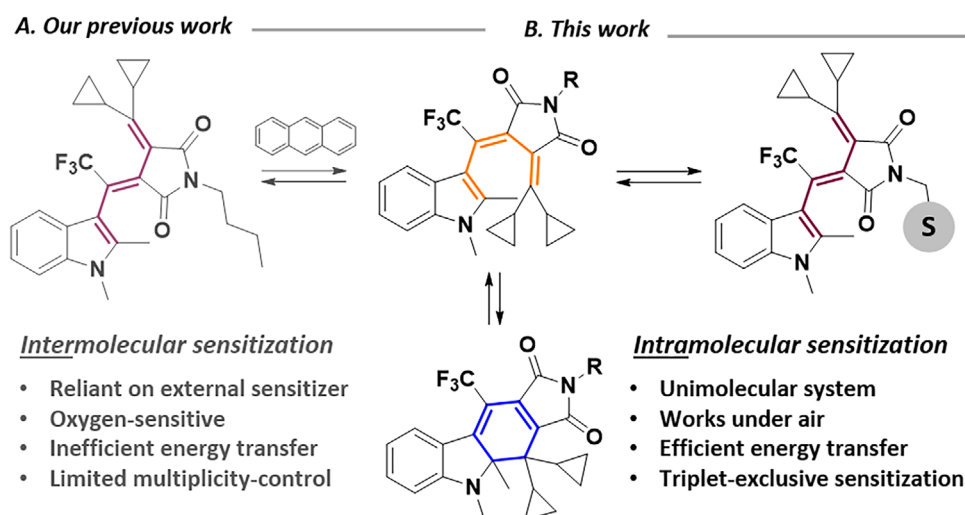
chemical instability, as exemplified by the oxidation of dihydrophenanthrene to a fully aromatic product. Therefore, effective substitution of the hexatriene core is crucial to enhance stability and reactivity. A promising solution is the use of fulgides,<sup>[28]</sup> which offer improved stability, tuneable reactivity, and structural versatility, making them valuable alternatives for achieving controlled multimodal reactivity in similar scaffolds (Scheme 1, bottom).

Fulgides are photoresponsive compounds that exhibit remarkable potential for applications in molecular switches and materials science, largely due to their ability to undergo reversible photochemical transformations.<sup>[29,30]</sup> One of their most intriguing features is their aptitude for three-state photo-switching. Like stilbenes, fulgides can undergo photoinduced double-bond isomerization or electrocyclic closure. We recently demonstrated that the interconversion between states in fulgides can be controlled by the multiplicity of the excited state.<sup>[27]</sup> Specifically, electrocyclic closure, cycloreversion, and Z-E double-bond isomerization occur via direct excitation of the singlet excited state, while E-Z double-bond isomerization proceeds via the triplet excited state. However, achieving a sufficient quantum yield of ISC to the triplet excited state is extremely rare in the case of fulgides. To compensate, fulgides rely on the use of an external triplet sensitizer (Scheme 3).

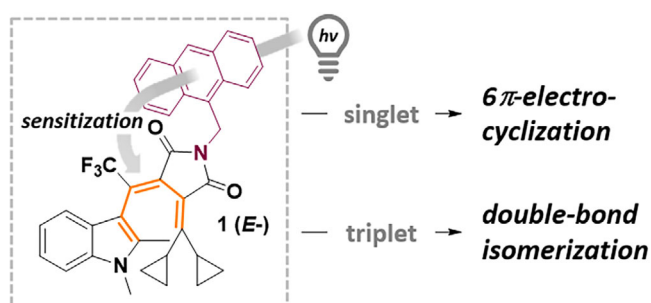
## 2. Results and Discussion

Reliance on the external sensitizer limits the application of the system to solution-based settings. To address this issue, we introduced anthracene, a previously utilized sensitizer,<sup>[27]</sup> into the scaffold via the imide functionality (Scheme 4). Its incorporation had little influence on ring-closing, opening, or Z- to E- isomerization, as the isomer ratios in PSSs and quantum yields for these transformations remained comparable to the intermolecular system (Table S1).

However, anthracene incorporation did have a significant impact on E- to Z- isomerization. In the original intermolecular system, E- to Z- isomerization yielded up to 90% of the Z-form upon exhaustive irradiation. However, it decreased dramatically to 30% in the intramolecular system. Such a marked decrease in Z-form formation must be attributed to the proximity of the sensitizer to the fulgimide core. Since the E-form undergoes two distinct reaction pathways based on excited-state multiplicity, its sensitization is highly attuned to the multiplicity of the energy transfer. By comparing the anthracene fluorescence in the inter- and intramolecular systems (Figure S7), we found that anthracene can act as both a singlet and triplet sensitizer. Notably, the fluorescence of anthracene was suppressed in the intramolecular system (Figure S8). However, upon increasing the integration time, weak vibronically structured emission characteristic of anthracene was detected, along with a broad emission associated with the fulgimide moiety. The latter emission could also be induced by selectively exciting the fulgimide absorption band. These observations suggest that electronic communication between the two molecular components occurs through



**Scheme 3.** Comparison of inter- and intramolecular variants of three-state fulgimide photoswitching; S = sensitizer.



**Scheme 4.** Multiplicity-dependent isomerizations of fulgimide 1. Note that we are aware of the incorrect description of the double bond configuration (E- instead of Z-); historically, trifluoromethyl was not present in the scaffold, but the fulgide nomenclature prevailed.

space, likely via Förster Resonance Energy Transfer (FRET), with anthracene primarily acting as a singlet sensitizer when covalently linked to fulgimide. To further support this conclusion, sensitization of fulgimide **1** was performed in the presence of an additional equivalent of external anthracene sensitizer, which increased the yield of the Z-form to 55% upon exhaustive irradiation. This result indicates that the Z/E isomer ratio is governed neither by steric effects of the intramolecular sensitizer nor by the fulgide triplet energy surface. Instead, it is determined solely by the excited state multiplicity of the sensitizer as perceived by the fulgide moiety.

This fact explains the low yield of sensitized Z-form generation in the intramolecular system, as the singlet state primarily generates the closed C-form. Therefore, in order to strictly control the multiplicity of the excited state, as well as its reactivity, efficiency, and yield, we set out to identify a more potent triplet-exclusive sensitizer, one that would minimize singlet sensitization while maximizing triplet energy transfer.

For that purpose, we focused on optimizing the sensitizer in the intermolecular system. The observed rate of E-Z isomerization serves as a key indicator of triplet sensitization efficiency, which is also a crucial parameter for the intramolecular system. The faster the observed rate of E-Z isomerization, the less sensi-

tive it is to any side reactivity originating from the singlet excited state.

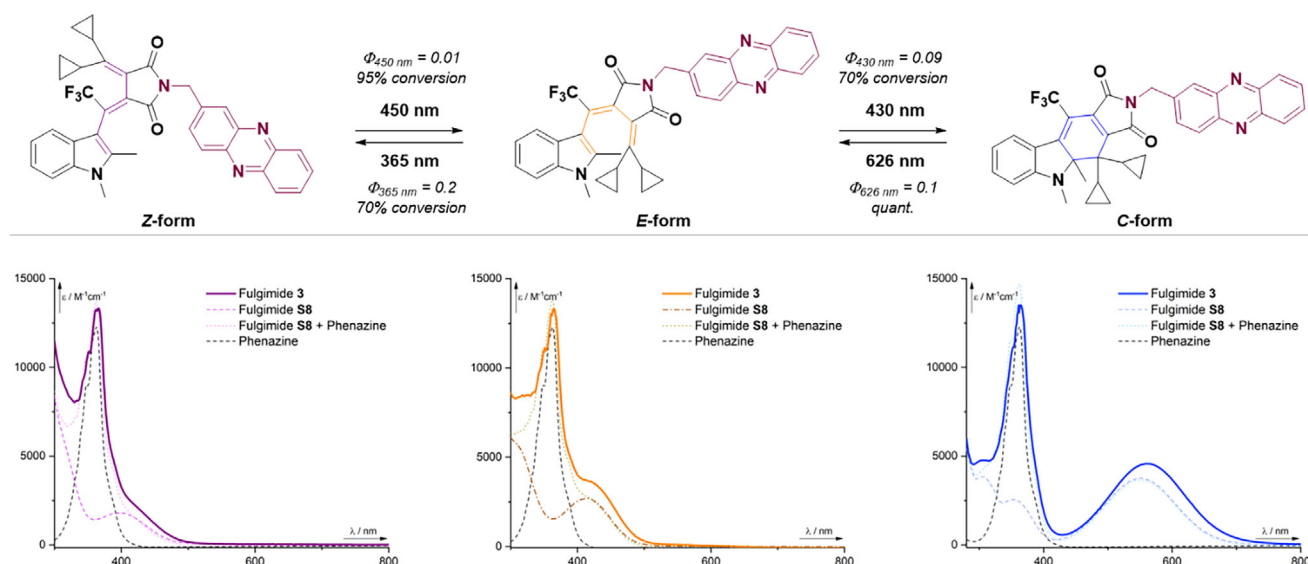
In our initial study, we utilized anthracene as a sensitizer due to its high ISC quantum yield and suitable triplet energy ( $\Phi_{ISC} = 0.71$ ,  $E_T = 178$  kJ/mol,  $\tau_s = 5.3$  ns).<sup>[31]</sup> One of the key factors typically optimized for enhancing the efficiency of triplet sensitizers is the ISC quantum yield. ISC is the process by which a molecule transitions from a singlet excited state to a triplet excited state. Therefore, a higher ISC quantum yield generally enhances triplet sensitizer efficiency. Intrigued by this association, we tested 9-bromoanthracene as an intermolecular sensitizer, leveraging the heavy-atom effect of the bromide substituent to enhance ISC ( $\Phi_{ISC} = 0.98$ )<sup>[31]</sup> and increase spin-orbit coupling.<sup>[32]</sup> Counterintuitively, however, the initial observed rate of Z-form generation during triplet-sensitized E-Z double-bond isomerization decreased by approximately 20% compared to anthracene (see the Sensitizer Optimization chapter in the Supporting Information). Despite its higher ISC quantum yield, 9-bromoanthracene exhibits a lower triplet excited-state energy ( $E_T = 173$  kJ/mol)<sup>[31]</sup> than its unsubstituted analogue, which might explain the reduced isomerization rate. Therefore, we utilized acridine, which has a higher triplet-state energy ( $E_T = 188$  kJ/mol),<sup>[31]</sup> as a sensitizer. Despite having a lower ISC quantum yield ( $\Phi_{ISC} = 0.82$ ), this change led to two-fold increase the initial observed rate of Z-form generation (Figure S23).

Though this is a marked improvement, it is important to realize that these parameters are bound to the intermolecular sensitization systems. The intramolecular sensitization of multiplicity-controlled multimodal systems presents a further challenge: the time scale of the energy transfer. As the sensitizer is held in close proximity to the acceptor within a single molecule, energy transfer can occur within just a few hundred picoseconds.<sup>[33]</sup> The singlet excited-state lifetime of acridine is 350 picoseconds, which suggests that the ISC rate competes with the singlet excited-state energy transfer, resulting in the formation of an undesired electrocyclic product.

To prevent this from occurring, we sought a triplet-exclusive sensitizer with the shortest possible singlet excited-state lifetime,







**Scheme 7.** Upper part: Photoinduced isomerization between three states of fulgimide 3. Bottom part: Absorption profile of all isomeric forms of fulgimide 3 in acetonitrile overlaid with phenazine, reference  $N_{(\text{imide})}$ -butyl-bearing fulgimide S8, and their sum.

pathways (Figures S24 and S25), strongly resembling the behavior of two separate chromophores.

Electrocyclization of fulgides occurs rapidly from the  $\pi, \pi^*$ -singlet excited state ( $\tau(S_1, E\text{-form}) = 1.5$  ps, Figure S26) of the *E*-form upon blue-light excitation, resulting in conversion to the closed isomer C ( $\Phi_{E \rightarrow C, 430\text{ nm}} = 9\%$ , 70% in PSS). The closed isomer can also be opened by red-light excitation into the  $\pi, \pi^*$ -singlet excited state ( $\tau(S_1, \text{closed form}) = 1.3$  ps, Figure S26), quantitatively restoring the initial *E*-isomer ( $\Phi_{C \rightarrow E, 626\text{ nm}} = 10\%$ ). Similar to previous observations,<sup>[34]</sup> electrocyclization can occur both in solution and in the solid state (Figure S21).

To elucidate the fate of electronically excited phenazine bound to the fulgide core, time-resolved absorption spectra were measured for all isomeric forms and unsubstituted phenazine. Upon excitation, unbound phenazine reaches the  $\pi, \pi^*$ -singlet excited state ( $S_1$ ,  $\tau(S_1) = 11$  ps), which in turn undergoes ISC toward a higher  $n, \pi^*$ -triplet excited state ( $T_2$ ,  $\tau(T_2) = 66$  ps, Figure S24). This state then rapidly undergoes internal conversion, reaching the lowest  $\pi, \pi^*$ -triplet excited state ( $T_1$ ), which, in the absence of an energy acceptor, is quenched by molecular oxygen ( $\tau(T_1, \text{aerated}) = 240$  ns, Figure S27). This relaxation pathway mirrors the previously documented behavior of a structurally similar acridine.<sup>[35,36]</sup>

A comparison of unsubstituted phenazine (Figure 1a) with the covalently bound fulgimide 3 (Figure 1b–d) shows that all isomeric forms of the fulgide core quench the triplet excited states of phenazine. Both the spectra of the *E*- and *Z*-forms (Figure 1b and c) highlight the high efficacy of the energy transfer, as even the short-lived  $n, \pi^*$ -state of phenazine is quenched to some extent ( $\tau(T_2)$  shortens from 66 to 42 ps, Figure S24). This result, together with the energy transfer from the  $\pi, \pi^*$ - $T_1$  state of phenazine, contributes to the highly effective sensitization of the fulgimide core. The photosensitization outcome is dictated by the geometry with the lowest energy (phantom triplet state), giving rise to the preferential generation of the *Z*-form.

Further, the time-resolved spectra help to unravel the smaller conversion to the *Z*-form compared to the intermolecular variant (70% versus 90%). Though the system is optimized to perform triplet-exclusive sensitization, a small percentage of phenazine's singlet excited state continued to sensitize the fulgide moiety to  $S_1$ . This is evident from the slightly decreased lifetime of the phenazine singlet excited state in 1 compared to phenazine alone (9 versus 11 ps, respectively) (Figure S24). This is in agreement with reported values for proximal intramolecular energy transfer.<sup>[37,38]</sup> This also explains the lower yield of the *Z*-form, as singlet reactivity leads to the reversal of the isomerization.

In the case of the closed form (Figure 1d), quenching of the excited states of phenazine proceeds similarly ( $\tau(S_1) = 9$  ps,  $\tau(T_2) = 42$  ps,  $\tau(T_1) = 10$  ns) (Figure S24 for  $S_1$  and  $T_2$ , Figure S27 for  $T_1$ ). However, the closed form shows no apparent triplet excited state reactivity. The newly apparent transient at around 610 nm corresponds to the singlet excited state of the closed form, formed by: (i) direct excitation of the fulgimide part by the 350 nm pump, (ii) singlet excited state energy transfer from phenazine.

To switch back to the *E*-form, the *Z*-*E* isomerization must be facilitated by direct excitation of the fulgide core through blue-light irradiation. Irradiating the tail of the  $\pi, \pi^*$ -absorption band ( $\Phi_{Z \rightarrow E, 450\text{ nm}} = 1\%$ ) proved the most efficient approach for *Z*-*E* isomerization, leaving only 5% of the *Z*-isomer in the mixture. Since the absorption spectra of the *Z*- and *E*-isomers almost completely overlap, blue-light irradiation also triggers the subsequent electrocyclization of the *E*-isomer. To prevent this scenario, dual irradiation with blue and red light can be employed. The additional red light induces electrocyclic opening of the closed form, restoring the *E*-form. Alternatively, red-light irradiation can be applied at a later stage, resulting in complete ring-opening and exclusive yielding of the *E*-isomer. Remarkably, the double-bond isomerization proceeds in both directions even in solid state (Figure S21).

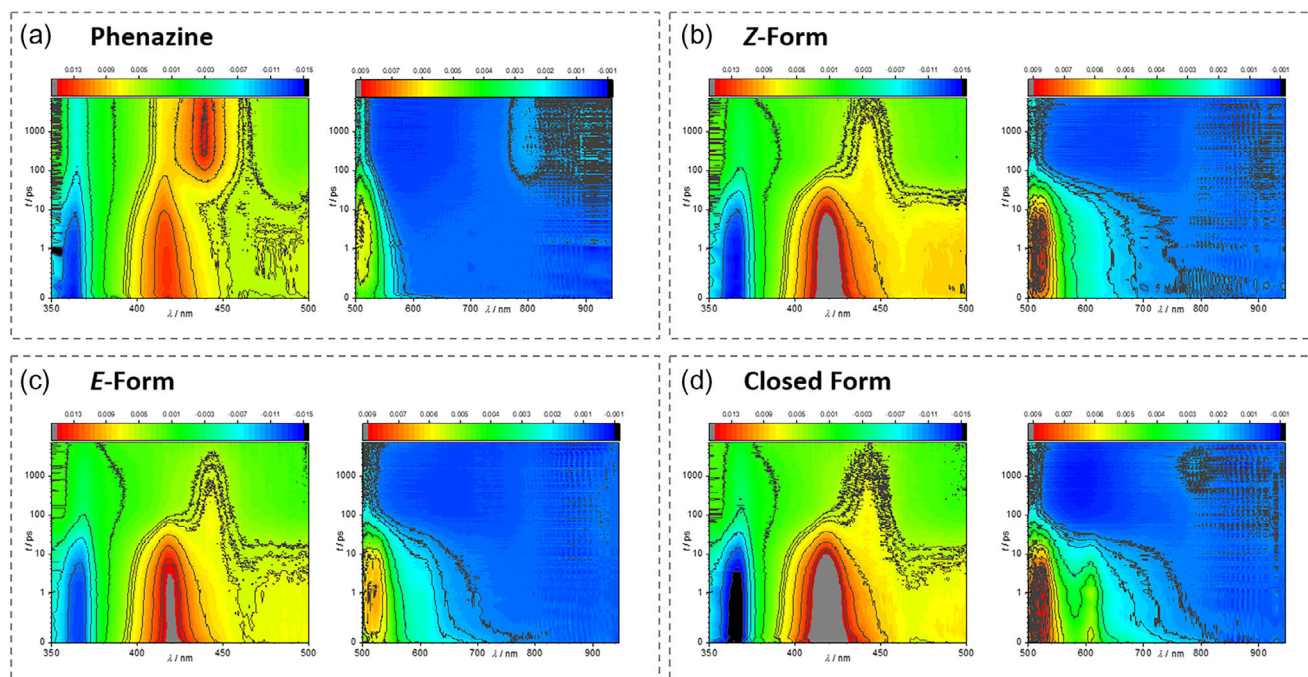


**Figure 1.** Time-resolved absorption spectra of (a) phenazine, (b) the Z-form, (c) the E-form, and (d) the closed form of fulgimide 3 in acetonitrile excited with 200 nJ pulse at 350 nm.

Another critical challenge in multiplicity-controlled multimodal systems is the need for inert atmospheric conditions that enable triplet-sensitized processes. Oxygen typically hinders triplet sensitization by quenching the triplet excited state of the sensitizer. The triplet excited state of a structurally similar anthracene is quenched with a rate constant of  $2.2 \times 10^9 \text{ M}^{-1}\text{s}^{-1}$  in acetonitrile at 298 K ( $C_{O_2} = 1.9 \times 10^{-3} \text{ M}$ ).<sup>[39,40]</sup> This corresponds to a triplet-state lifetime of up to 240 ns, a value that is in agreement with our observed quenching of  $T_1$  of phenazine by molecular oxygen ( $\tau(T_1, \text{aerated}) = 240 \text{ ns}$ , Figure S27). Consequently, processes occurring faster than this timescale should be largely insensitive to oxygen, allowing triplet-sensitized reactions to proceed under ambient conditions without any loss of efficiency. Indeed, the rapid kinetics of phenazine ISC and E-Z double-bond isomerization (both  $<50 \text{ ns}$ ) explain why triplet sensitization remains effective even in the presence of oxygen, eliminating the need for a strictly inert atmosphere.

### 3. Conclusion

Multiplicity-controlled reactivity is a well-established principle that enables the precise manipulation of chemical reactivity to achieve the formation of desired products.<sup>[41–47]</sup> In this study, we present an extension to the existing multimodal photochemistry toolkit, expanding its scope to include reversible and/or unimolecular reactivity. By introducing phenazine as an optimized triplet-exclusive sensitizer, we achieved selective triplet-state sensitization of the fulgide scaffold. We demonstrated that both photoswitching modes—electrocyclization and E-Z isomerization—proceed with a high efficiency, yielding quantum efficiencies comparable to similar fulgide-based systems.

Furthermore, intramolecular triplet sensitization enables high yields of the desired Z-isomer, eliminating the need for inert conditions. These advancements not only streamline the experimental protocol but also broaden the potential application of this photochemical system to real-world environments, such as photopharmacology in solution or optical data storage in a solid phase.

In addition to showcasing the advantages of our unique, multiplicity-controlled, three-state photoswitching system, this work provides valuable insights into the rational selection of triplet-exclusive sensitizers for cases requiring strict control over excited-state multiplicity. Having an exceptionally short singlet excited-state lifetime is equally important as having a suitable triplet excited-state energy. Maintaining both is crucial for ensuring exclusive reactivity originating from the triplet excited state. Finally, we believe that the presented work could reignite interest in multiplicity-controlled reactivity beyond the field of photochromism, providing a powerful tool to control reaction outcomes through external inputs in other areas of photochemistry.

### 4. Experimental Section

**Reagents:** All grade-quality reagents and dry solvents were commercially available and used without any further purification. They were purchased from Merck (Germany), Fluorochem Ltd. (United Kingdom), TCI (Japan), Penta Chemicals (Czech Republic), and Thermo Fisher scientific (Belgium).

**Instrumentation:** NMR spectra were recorded on Bruker Avance III HD 400 MHz and Bruker Avance III HD 400 MHz Prodigy

spectrometers. High-resolution mass spectra were recorded on an LTQ Orbitrap XL hybrid FT mass spectrometer equipped with a linear ion trap MS and the Orbitrap mass analyzer. Transient absorption experiments were carried out using commercially available apparatus from Ultrafast Systems. Absorption and emission spectra were collected on Agilent Cary 8454 and Horiba Duetta spectrometer. Irradiation was performed by custom-designed LED light sources (for spectral profiles see SI) or by Horiba Duetta spectrometer. LCMS analysis was performed on LC-MS-2020 system from Shimadzu Corporation. Further details are provided in [Supporting Information](#).

**Synthesis:** Starting materials were prepared following previously described procedures.<sup>[27,48–50]</sup> Fulgimides **1** and **3** were synthesized from the lactone precursor **2** and the corresponding amine, according to the following protocol:<sup>[27]</sup>

Lactone **2** (50 mg, 0.11 mmol, 1 equiv.) was dissolved in dry DMF (2 mL) and sodium hydride (60% dispersion in paraffin oil, 6.7 mg, 0.17 mmol, 1.4 equiv.) was added in one portion. The reaction was monitored by TLC. Once the starting material was consumed (typically 1–2 hours), hexafluorophosphate azabenzotriazole tetramethyl uronium (HATU) (51 mg, 0.13 mmol, 1.2 equiv.) was added in one portion. After 5 minutes, amine (1.3 equiv.) was added, and the reaction was stirred for one hour. Subsequently, the reaction was cooled to 0 °C, and a second portion of sodium hydride (60% dispersion in paraffin oil, 9 mg, 0.22 mmol, 2 equiv.) was added. The reaction progress was monitored by LCMS. Once the starting material was consumed (typically after 30 minutes), the reaction was terminated by adding HATU (25.5 mg, 0.17 mmol, 0.6 equiv.). The reaction mixture was stirred for 5 minutes, after which the solvent was evaporated under reduced pressure. The crude product was filtered through a pad of silica (eluted with either DCM or ethyl acetate, depending on the maleimide *N*-substituent) and then purified by semi-preparative HPLC yielding the target fulgimide in its *Z*-form.

**Fulgimide 1:** Following the abovementioned procedure, utilizing anthracen-9-ylmethanamine **S4**, the target compound **1** was prepared as a yellow solid (43 mg, 69%). Filtration through pad of silica was performed by DCM. <sup>1</sup>H NMR (401 MHz, CD<sub>2</sub>Cl<sub>2</sub>) δ 8.27–8.17 (m, 2H), 8.13 (d, *J* = 9.0 Hz, 1H), 8.03 (s, 1H), 7.89–7.82 (m, 2H), 7.66 (bs, 1H), 7.30 (d, *J* = 8.1 Hz, 1H), 7.28 (bs, 1H), 7.17–7.07 (m, 1H), 6.98 (bs, 1H), 4.90 (d, *J* = 14.9 Hz, 1H), 4.83 (d, *J* = 15.0 Hz, 1H), 3.70 (s, 3H), 3.32 (s, 1H), 2.65–1.94 (m, 2H), 1.64–1.58 (m, 1H), 1.25–0.97 (m, 6H), 0.96–0.47 (m, 1H). <sup>13</sup>C NMR (101 MHz, CD<sub>2</sub>Cl<sub>2</sub>) δ 167.37, 165.72, 144.16, 143.98, 143.65, 143.36, 139.08, 136.99, 131.19, 130.89, 130.80, 130.42, 130.09, 128.46, 121.30, 120.21, 109.42, 104.11, 41.69, 30.19, 17.23, 15.39, 11.50, 11.30–8.35 (m). <sup>19</sup>F NMR (377 MHz, CD<sub>2</sub>Cl<sub>2</sub>) δ -63.63–-64.59 (m). HRMS (ESI+): calculated for C<sub>36</sub>H<sub>30</sub>O<sub>2</sub>N<sub>4</sub>F<sub>3</sub> [M + H]<sup>+</sup> 607.23154; found 607.23138.

**Fulgimide 3:** Prior to the one-pot transformation, phenazine-2-ylmethanamine **4** was prepared. Under a nitrogen atmosphere, 2-(azidomethyl)phenazine **S7** (170 mg, 0.72 mmol, 1 equiv.) was dissolved in dry THF (3 mL) and cooled to 0 °C. Triphenylphosphine (210 mg, 0.80 mmol, 1.1 equiv.) was added in one portion, and the reaction was heated to RT and reacted for 2 hour after which water (22 µL, 22 mg, 1.23 mmol, 1.7 equiv.) was added and left to react overnight. The reaction mixture was treated with diethyl ether (3 mL) and a few drops of 1 M HCl to form a precipitate. The precipitate was collected, dissolved in water, and basified using 1 M NaOH to reach pH 10. The target compound was extracted to ethyl acetate, the organic layer was washed with brine, dried over MgSO<sub>4</sub>, and evaporated to give 74 mg of yellow solid as a 9:1 mixture (based on <sup>1</sup>H NMR) of the title compound (corresponds to 67 mg, 44%) and

triphenylphosphine oxide. This mixture was used without further purification in the following step.

Further, following the abovementioned procedure, utilizing amine **4**, the target compound **3** was prepared as a yellow solid (47 mg, 69%). Filtration through pad of silica was performed by ethyl acetate. <sup>1</sup>H NMR (401 MHz, CD<sub>2</sub>Cl<sub>2</sub>) δ 8.27–8.17 (m, 2H), 8.13 (d, *J* = 9.0 Hz, 1H), 8.03 (s, 1H), 7.89–7.82 (m, 2H), 7.66 (bs, 1H), 7.30 (d, *J* = 8.1 Hz, 1H), 7.28 (bs, 1H), 7.17–7.07 (m, 1H), 6.98 (bs, 1H), 4.90 (d, *J* = 14.9 Hz, 1H), 4.83 (d, *J* = 15.0 Hz, 1H), 3.70 (s, 3H), 3.32 (s, 1H), 2.65–1.94 (m, 2H), 1.64–1.58 (m, 1H), 1.25–0.97 (m, 6H), 0.96–0.47 (m, 1H). <sup>13</sup>C NMR (101 MHz, CD<sub>2</sub>Cl<sub>2</sub>) δ 167.37, 165.72, 144.16, 143.98, 143.65, 143.36, 139.08, 136.99, 131.19, 130.89, 130.80, 130.42, 130.09, 128.46, 121.30, 120.21, 109.42, 104.11, 41.69, 30.19, 17.23, 15.39, 11.50, 11.30–8.35 (m). <sup>19</sup>F NMR (377 MHz, CD<sub>2</sub>Cl<sub>2</sub>) δ -63.63 – -64.59 (m). HRMS (ESI+): calculated for C<sub>36</sub>H<sub>30</sub>O<sub>2</sub>N<sub>4</sub>F<sub>3</sub> [M + H]<sup>+</sup> 607.23154; found 607.23138.

**Data evaluation:** The compositions of PSSs of **1** and **3** was determined based on HPLC PDA signals at corresponding isosbestic points. The **determination of pure spectra** was carried out as follows: the spectrum of the synthesized fulgimide corresponds to the *Z*-form. Irradiation of the fulgimide by 450 nm followed by 626 nm resulted in a mixture of *Z*- and *E*-forms, from which the spectrum of the pure *E*-form was determined using the Lambert-Beer law by subtracting the residual absorbance of the *Z*-form. Further irradiation of this mixture produced a ternary combination of *Z*-, *E*-, and closed isomers, from which the spectrum of the pure closed isomer was determined by subtracting the *Z*- and *E*-residual absorbances. **Quantum yields** were calculated following the procedure published by Börjesson et. al.<sup>[51]</sup> **Photon fluxes** of the irradiation sources were determined using actinometry in accordance with the procedure published by Reinfelds et. al.<sup>[52]</sup>

Further details are provided in the [Supporting Information](#).

## Supporting Information

Supplementary Figures and Schemes, detailed synthetic procedure of intermediate compounds, NMR and HRMS spectra, photophysical properties and their evaluation (both steady-state and time resolved), spectral data for **1,3**, and **S8**. The authors have cited additional references within the Supporting Information.<sup>[48–55]</sup>

## Acknowledgments

J.C. expresses gratitude to Eva Bednářová for her valuable insights and contributions to this project. All the authors express their gratitude to Michael FitzGerald for editing the manuscript. This research was supported by Ministerstvo Školství, Mládeže a Tělovýchovy.

Open access publishing facilitated by Ústav organické chemie a biochemie Akademie věd České republiky, as part of the Wiley - CzechELib agreement.

## Conflicts of Interests

The authors declare no conflicts of interest.



**Keywords:** fulgide · fulgimide · photochemistry · photochromism · sensitization

- [1] D. Bourissou, O. Guerret, F. P. Gabbaï, G. Bertrand, *Chem. Rev.* **2000**, *100*, 39.
- [2] P. de Frémont, N. Marion, S. P. Nolan, *Coord. Chem. Rev.* **2009**, *253*, 862.
- [3] D. L. S. Brahms, W. P. Dailey, *Chem. Rev.* **1996**, *96*, 1585.
- [4] S. Mai, L. González, *Angew. Chem., Int. Ed.* **2020**, *59*, 16832.
- [5] D. H. Waldeck, *Chem. Rev.* **1991**, *91*, 415.
- [6] J. M. Rodier, A. B. Myers, *J. Am. Chem. Soc.* **1993**, *115*, 10791.
- [7] H. Meier, *Angew. Chem., Int. Ed.* **1992**, *31*, 1399.
- [8] N. J. Turro, V. Ramamurthy, J. C. Scaiano, *Modern Molecular Photochemistry of Organic Molecules*, University Science Books, **2010**.
- [9] F. B. Mallory, C. S. Wood, J. T. Gordon, L. C. Lindquist, M. L. Savitz, *J. Am. Chem. Soc.* **1962**, *84*, 4361.
- [10] F. B. Mallory, C. S. Wood, J. T. Gordon, *J. Am. Chem. Soc.* **1964**, *86*, 3094.
- [11] Q. Zhou, G. Kukier, I. Gordiy, R. Hoffmann, J. I. Seeman, K. N. Houk, *J. Org. Chem.* **2024**, *89*, 1018.
- [12] G. S. Hammond, J. Saltiel, A. A. Lamola, N. J. Turro, J. S. Bradshaw, D. O. Cowan, R. C. Counsell, V. Vogt, C. Dalton, *J. Am. Chem. Soc.* **1964**, *86*, 3197.
- [13] M. Reimann, E. Teichmann, S. Hecht, M. Kaupp, *J. Phys. Chem. Lett.* **2022**, *13*, 10882.
- [14] K. Kuntze, J. Isokuortti, J. J. van der Wal, T. Laaksonen, S. Crespi, N. A. Durandin, A. Priimagi, *Chem. Sci.* **2024**, *15*, 11684.
- [15] W.-G. Han, T. Lovell, T. Liu, L. Noodleman, *ChemPhysChem* **2002**, *3*, 167.
- [16] V. D. Vachev, J. H. Frederick, B. A. Grishanin, V. N. Zadkov, N. I. Koroteev, *Chem. Phys. Lett.* **1993**, *215*, 306.
- [17] S. T. Repinec, R. J. Sension, R. M. Hochstrasser, *Ber Bunsenges Phys Chem* **1991**, *95*, 248.
- [18] V. Sundström, T. Gillbro, *Chem. Phys. Lett.* **1984**, *109*, 538.
- [19] J. Saltiel, S. Ganapathy, C. Werking, *J. Phys. Chem.* **1987**, *91*, 2755.
- [20] T. Arai, T. Karatsu, H. Sakuragi, K. Tokumari, *Tetrahedron Lett.* **1983**, *24*, 2873.
- [21] H. Goerner, D. Schulte-Frohlinde, *J. Phys. Chem.* **1981**, *85*, 1835.
- [22] F. W. Langkilde, R. Wilbrandt, A. M. Brouwer, F. Negri, F. Zerbetto, G. Orlandi, *J. Phys. Chem.* **1994**, *98*, 2254.
- [23] K. Nakatani, H. Sato, R. Fukuda, *Phys. Chem. Chem. Phys.* **2022**, *24*, 1712.
- [24] J. Saltiel, G. R. Marchand, E. Kirkor-Kaminska, W. K. Smothers, W. B. Mueller, J. L. Charlton, *J. Am. Chem. Soc.* **1984**, *106*, 3144.
- [25] J. Saltiel, A. D. Rousseau, B. Thomas, *J. Am. Chem. Soc.* **1983**, *105*, 7631.
- [26] J. Saltiel, *J. Am. Chem. Soc.* **1968**, *90*, 6394.
- [27] J. Copko, T. Slanina, *Chem. Commun.* **2024**, *60*, 3774.
- [28] Y. Yokoyama, *Chem. Rev.* **2000**, *100*, 1717.
- [29] D. Lachmann, R. Lahmy, B. König, *Eur. J. Org. Chem.* **2019**, *2019*, 5018.
- [30] S. Nigel Corns, S. M. Partington, A. D. Towns, *Color. Technol.* **2009**, *125*, 249.
- [31] M. Montalti, A. Credi, L. Prodi, M. T. Gandolfi, *Handbook of Photochemistry*, CRC Press, Boca Raton, **2006**.
- [32] J. C. Koziar, D. O. Cowan, *Acc. Chem. Res.* **1978**, *11*, 334.
- [33] P. J. Wagner, P. Klán, *J. Am. Chem. Soc.* **1999**, *121*, 9626.
- [34] Y. Jiao, R. Yang, Y. Luo, L. Liu, B. Xu, W. Tian, *CCS Chemistry* **2021**, *4*, 132.
- [35] S. L. Shapiro, K. R. Winn, *J. Chem. Phys.* **1980**, *73*, 5958.
- [36] L. A. Diverdi, M. R. Topp, *J. Phys. Chem.* **1984**, *88*, 3447.
- [37] R. W. Anderson Jr., R. M. Hochstrasser, H. Lutz, G. W. Scott, *J. Chem. Phys.* **1974**, *61*, 2500.
- [38] J. Saltiel, P. T. Shannon, O. C. Zafiriou, A. K. Uriarte, *J. Am. Chem. Soc.* **1980**, *102*, 6799.
- [39] F. Wilkinson, A. A. Abdel-Shafi, *J. Phys. Chem. A* **1997**, *101*, 5509.
- [40] A. A. Abdel-Shafi, D. R. Worrall, *J. Photochem. Photobiol. A* **2005**, *172*, 170.
- [41] Y. Inoue, *Chem. Rev.* **1992**, *92*, 741.
- [42] A. G. Griesbeck, M. Abe, S. Bondock, *Acc. Chem. Res.* **2004**, *37*, 919.
- [43] S. Bondock, A. G. Griesbeck, *Int. J. Photoenergy* **2005**, *7*, 830205.
- [44] R. Jahjah, A. Gassama, V. Bulach, C. Suzuki, M. Abe, N. Hoffmann, A. Martinez, J.-M. Nuzillard, *Chem. Eur. J.* **2010**, *16*, 3341.
- [45] M. Leverenz, C. Merten, A. Dreuw, T. Bach, *J. Am. Chem. Soc.* **2019**, *141*, 20053.
- [46] A. Griesbeck, S. Bozkus, *Chimia* **2021**, *75*, 868.
- [47] P. Yan, S. Stegbauer, Q. Wu, E. Kolodzeiski, C. J. Stein, P. Lu, T. Bach, *Angew. Chem., Int. Ed.* **2024**, *63*, e202318126.
- [48] A. Borisov, J. Y. C. Lim, A. Brown, K. E. Christensen, A. L. Thompson, M. D. Smith, P. D. Beer, *Chem. Commun.* **2017**, *53*, 2483.
- [49] J. Singh, N. Steck, D. De, A. Hofer, A. Ripp, I. Captain, M. Keller, P. A. Wender, R. Bhandari, H. J. Jessen, *Angew. Chem., Int. Ed.* **2019**, *58*, 3928.
- [50] N. L. Maidwell, M. R. Rezai, C. A. Roeschlaub, P. G. Sammes, *J. Chem. Soc., Perkin Trans.* **2000**, *1*, 1541.
- [51] K. Stranius, K. Börjesson, *Sci. Rep.* **2017**, *7*, 41145.
- [52] M. Reinfelds, V. Hermanns, T. Halbritter, J. Wachtveitl, M. Braun, T. Slanina, A. Heckel, *ChemPhotoChem* **2019**, *3*, 441.
- [53] C. Slavov, H. Hartmann, J. Wachtveitl, *Anal. Chem.* **2015**, *87*, 2328.
- [54] M. N. Polyanskiy, *Sci Data* **2024**, *11*, 94.
- [55] J. E. Bertie, Z. Lan, *J. Phys. Chem. B* **1997**, *101*, 4111.

Manuscript received: February 20, 2025

Revised manuscript received: March 28, 2025

Version of record online: April 17, 2025